International Journal of Biology and Life Sciences
ISSN: 2957-9511 | Vol. 1, No. 1, 2022

Investigation of the interaction between glucose-6-phosphate dehydrogenase and ATA-inhibitor by molecular docking and molecular dynamics simulation

Kun Cao[1], Ruonan Wang[2], Ruixue Li[1], Xingdong Xiong[1], Xinguang Liu[1, *]

[1] Guangdong Key Laboratory of Medical Molecular Diagnostics, Institute of Aging Research, Institute of Biochemistry & Molecular Biology, Guangdong Medical University, Dongguan 523808, China
[2] Scientific Research Platform Service Management Center, Guangdong Medical University, Dongguan 523808, China
[*] **Corresponding author**: Xinguang Liu (Email: xgliu@gdmu.edu.cn)

Abstract: Human glucose-6-phosphate dehydrogenase (G6PD) is a kind of polymerase, which can bind cofactors β-D-glucose-6-phosphate (G6P) and catalyzes NADP+ to produce NADPH. Therefore, G6PD plays a crucial role in maintaining reduced glutathione to protect cells from oxidative stress disorders. Aurine tricarboxylic acid (ATA) is a potential metal binding inhibitor. Here, we found that G6P and ATA have a common potential binding site in the G6PD receptor conformation through molecular docking. The results of molecular dynamics (MD) simulation showed that, compared with apo-G6PD, G6P-G6PD and ATA-G6PD had lower root mean square deviation (RMSD), radius of gyration (Rg), and solvent accessible surface area (SASA), indicating that binding ligand molecules could promote the overall conformation of G6PD to be more stable. These results suggest that ATA may compete for the binding sites of G6P, thereby inhibiting the catalytic function of G6PD. This study revealed the mechanism of interaction between ATA inhibitors and G6PD at the atomic conformation level, providing a theoretical basis for investigating the effects of cellular oxidative stress.

Keywords: Molecular docking; Molecular dynamics simulation; Glucose-6-phosphate dehydrogenase; Inhibitor; Stability.

1. Introduction

Human glucose-6-phosphate dehydrogenase plays a catalytic role in the first step of pentose phosphate pathway, converting G6P into 6-phosphate gluconate lactone, and reducing $NADP^+$ to NAPDH [1-3]. G6PD deficiency is one of the most common human enzyme deficiencies. Red blood cells are particularly vulnerable to G6PD deficiency because they lack mitochondria. Human G6PD deficiency will cause red blood cells to be exposed to oxidants and lead to hemolytic anemia [4-7]. The lack of G6PD is mainly reflected in human beings in malaria endemic areas [8-10]. It has been reported that the overexpression of G6PD is also related to the pathogenesis of human cancer [11,12]. Therefore, the precise balance of G6PD expression level and activity in human body is crucial to cell viability.

Aurine tricarboxylic acid can form stable free radicals to inhibit protein nucleic acid interaction [13-15]. It has been reported that ATA can inhibit the binding of G6P and protease. This study will reveal the mechanism of ATA inhibiting the binding of G6PD and G6P at the atomic level through molecular docking and molecular dynamics simulation.

2. Material and methods

2.1. Molecular Docking

In this study, G6PD (PDB code: 7sni) was used as the receptor protein, G6P and ATA inhibitors were used as ligand molecules, and Autodock vina software was used (https://vina.scripps.edu/) to perform molecular docking. G6P and G6PD receptor (523 amino acid residues) were from RCSB protein database website (https://www.rcsb.org/), ATA inhibitor molecules (C22H14O9·3NH3) from PubChem database (https://pubchem.ncbi.nlm.nih.gov/).

2.2. Molecular Dynamics Simulation

In recent years, MD simulations have been widely used to study the interactions between protein to ligands, protein to protein [16]. In this study, three independent simulation systems have been constructed through Gromacs 2020.4 software, namely apo-G6PD, ATA-G6PD, and G6P-G6PD. According to the literature, although the complex crystal of G6P and G6PD has been revealed [3], there is no research on the influence of G6P binding on the conformation of G6PD protein at the atomic level, so it is necessary to simulate G6P-G6PD. Next, MD simulations with a total time of 100 ns were performed on the complexes of G6PD and different ligands. The amber99sb-ildn force field and SPC water model were used. The structure of the protein complex was placed in a cubic periodic box as the initial conformation, and the minimum distance between it and the box boundary was set to 1.2 nm. The periodic boundary conditions of the simulation system were applicable to the X, Y, Z directions. To neutralize the charge of the protein system, 0.15 mol/L NaCl salt solution was added to the system. The leapfrog algorithm was used to calculate the motion of each atom, and the particle mesh Ewald algorithm was used to calculate the electrostatic interaction energy [17]. In order to make the simulation system more reasonable, 400 steps of energy minimization should be carried out by the steepest descent method before the formal dynamics simulation, and 50 ps position constraint simulation should be carried out for each simulation system. The initial velocity of the simulation system was set as a random initial velocity.

3. Results

3.1. Molecular Docking between G6PD and Ligands

The ligands and G6PD receptor were predicted by semi-flexible docking. We set the active center residue as the flexible residue region, and further performed docking verification by autodock vina. The results showed that the docking energy of the two ligands was -19.96 and -18.66 respectively (Fig. 1A), indicating that the reliability trends of the docking results of the two ligands were consistent.

The ligand and G6PD receptor were predicted by semi flexible docking. We set the active center residue as the flexible residue region, and further performed docking verification by autodock vina. The results showed that the docking energy of the two ligands was -19.96 and -18.66 respectively (Fig. 1A), indicating that the reliability trends of the docking results of the two ligands were consistent.

In the crystal results of G6PD, the protein mainly bound to G6P through 12 amino acid residues [3], of which 10 residues were successfully docked by autodock vina software, and only Phe237 and Phe241 failed to bond. The results showed that the residues such as Lys171, His201, Tyr202, Lys205, Glu239, Asp258, His263, Lys360, Arg365, and Gln395 (Fig. 1B) that bound G6P in the form of van der Waals force, hydrogen bond, salt bridge, etc., indicated that the G6P binding sites obtained by docking were highly consistent with those expressed by crystallography. This implied that the docking results of ATA were reliable. The residues of ATA inhibitor and G6PD in the form of van der Waals force, hydrogen bond, salt bridge or conjugated π bond were: Lys47, Lys171, His201, Lys205, Phe237, Arg365, Gln395, and Tyr437 (Fig. 1C). These results suggest that the binding sites of G6P and ATA inhibitors and G6PD respectively belong to the same active center, and the two ligands may have the same binding sites: Lys171, His201, Lys205, Arg365, and Gln395.

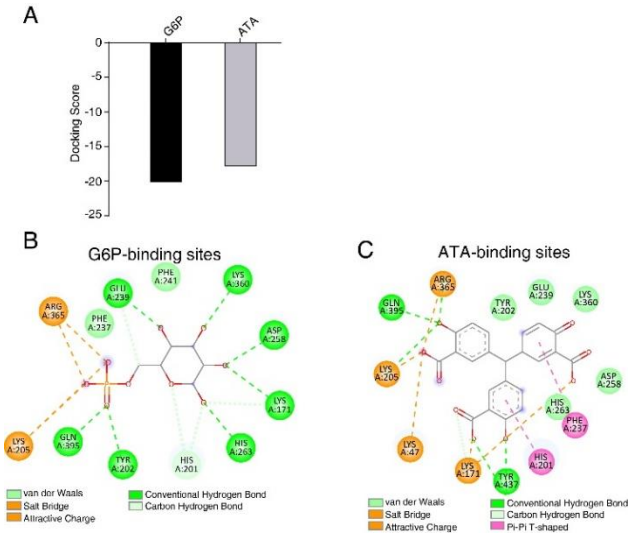

Figure 1. Molecular docking between G6PD and ligand molecules. (A) molecular docking score; (B) G6P binding sites; (C) ATA inhibitor binding sites.

3.2. Atomic Expression of Protein Conformation Change

The MD simulation of apo-G6PD, G6P-G6PD and ATA-G6PD was performed for 100 ns respectively through Gromacs software. The results showed that the RMSD value of apo-G6PD could not reach the equilibrium state within the simulation time of 100 ns (Fig. 2A). The RMSD of G6P-G6PD (positive control) entered the equilibrium state from 50 ns, while the RMSD trend of ATA-G6PD was consistent with that of the positive control.

To evaluate the fluctuation of protein α-C relative to its average position, we calculated the RMSF value of each c atom in the 50-80 ns equilibrium time. The RMSF values corresponding to a large number of amino acid residues in apo-G6PD were significantly higher than those of G6P-G6PD and ATA-G6PD, and the overall trend of the RMSF values of these two complexes was consistent (Fig. 2B). In order to calculate the fluctuation of ligand binding site residues, the RMSF values of representative residues Lys171, Lys205, His263, Arg365, and Gln395 (Fig. 2C) were separately calculated. The results showed that, compared with apo-G6PD, the RMSF values of residues corresponding to ATA-G6PD and G6P-G6PD were significantly reduced. These results further confirmed that the binding sites of G6P or ATA inhibitors were basically the same, indicated that ATA inhibitors may compete for the binding sites of G6P.

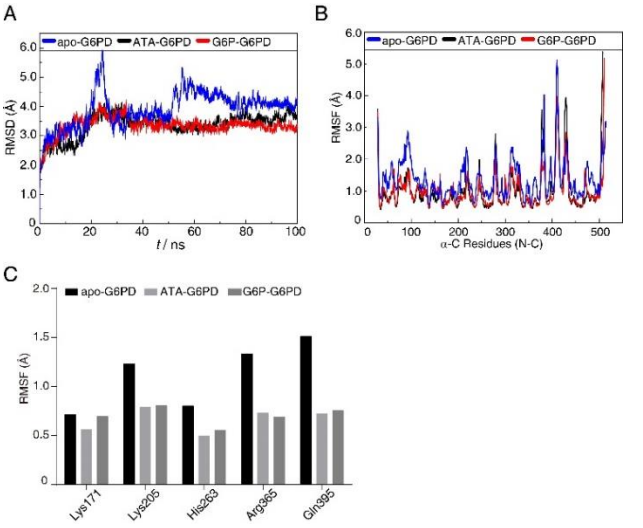

Figure 2. Atomic representation of protein structure change in MD systems. (A) The evolution of RMSD value with time; (B) The evolution of RMSF value with time; (C) Comparison of RMSF fluctuations of common binding sites residues of two ligands.

3.3. SASA analysis of protein conformation

According to the calculation results of 100 ns protein simulation (Fig. 3A), the average SASA of apo-G6PD was 248.2 nm2, in contrast to that of ATA-G6P and G6P-G6PD, which were reduced to 239.9 nm2 and 242.5 nm2. In addition, according to gmx make_ndx tool defined Lys171, Lys205, His263, Arg365, and Gln395 as a single component, and calculated their SASA values. The results showed that the SASA values of the binding sites corresponding to ATA-G6P and G6P-G6PD were 9.55 nm2 and 10.21 nm2 respectively (Fig. 3B), significantly lower than the 14.51 nm2 data corresponding to apo-G6PD. These results indicated that the change trend of SASA data was consistent with RMSD and RMSF values, suggesting that the overall conformation of apo-G6PD protein was relatively loose, and the ligand helped to increase the conformation stability of G6PD protein.

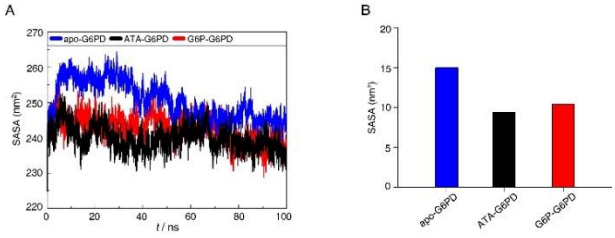

Figure 3. Display of protein SASA values in three simulation systems. (A) Evolution of overall SASA value of protein conformation with time; (B) SASA statistics of representative residues of G6PD protein.

3.4. Secondary Structure Changes of apo-G6PD and its Ligand Complexes

To identify the evolution of the secondary structure of apo-G6PD, ATA-G6P and G6P-G6PD with simulation time, we analyzed the contents of each component of the protein secondary structure through the do_dssp tool. Compared with apo-G6PD, the secondary structure contents of ATA-G6P and G6P-G6PD have changed greatly. In the apo-G6P conformation, 79 amino acid residues form β-turn and 131 residues form Helix (Fig. 4A); However, in the conformation of ATA-G6P and G6P-G6PD, the number of residues forming β-turn was 74 and 76 respectively, and the number of residues forming helix was 137 and 135 respectively (Fig. 4B-4C). These data indicated that ligand molecules will induce the β-turn contents in apo-G6PD conformation to change to helix.

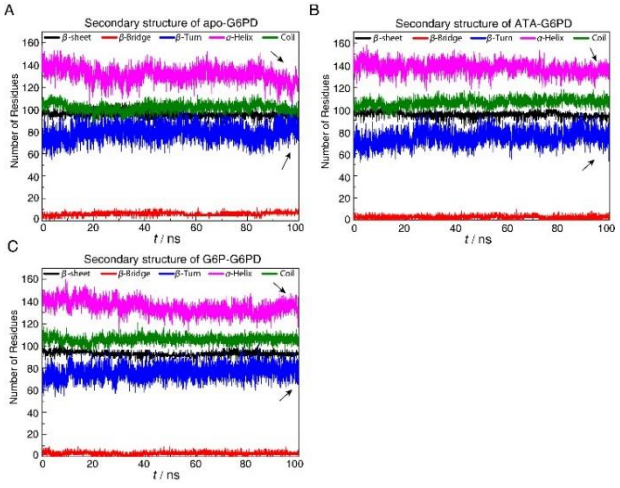

Figure 4. The main component contents of secondary structure of G6PD in three MD simulations. The secondary structures of apo-G6PD (A), ATA-G6PD (B), and G6P-G6PD (C) were shown in detail: -sheet, -bridge, -turn, -helix and coil. Y-axis represents the numbers of residues in each component.

4. Discussion

Human glucose-6-phosphate dehydrogenase plays a catalytic role in pentose phosphate pathway, and the production of NADPH in cells mainly depends on G6PD activity [19]. According to some research reports, the crystal structure of G6PD was mainly composed of monomers, dimers, and tetramers, which provided important insights for biochemical study of the action mode of the enzyme [20]. However, the overexpression of G6PD in cancer cells has been confirmed to be related to the pathogenesis of human cancer. Therefore, in this study, we investigated that ATA inhibitors can specifically compete for G6P binding sites. Horikoshi et al. recently reported G6PD mutants of class I (P396L, R393H, V394L and F381L), and the activity of mutants was only 10% of that of wild type [18]. These results fully showed that G6P ligands were crucial for G6PD to play an enzyme activity. However, we confirmed that ATA and G6P have the similar binding sites, among which Lys171, Lys205, His263, Arg365, and Gln395 have the highest contribution to ligand binding. Further MD simulation results showed that ATA-G6P and G6P-G6PD have lower RMSD and RMSF values compared with apo-G6PD, indicating that the composite has higher stability. The binding of ligands might cause the hydrophobic groups of the active center to be embedded in the protein, which will affect the proportion of each component of the G6PD secondary structure, and promoted the protein to be allosteric. In conclusion, we investigated the potential interaction mechanism of ATA and G6PD at the atomic level, providing a theoretical basis for inhibiting the activity of G6PD in tumor cells.

Acknowledgments

This work was supported by: Basic and Applied Basic Research Fund of Guangdong Province (2019A1515110659, 2021B1515140058, 2022A1515010191); Key project of universities in Guangdong Province (2022ZDZX2023); Scientific Research Initiation Fund for Doctoral Degree Personnel of Guangdong Medical University and Program of Natural Science (B2019018, GDMUM2020016); Discipline Construction Project of Guangdong Medical University (4SG21008G).

References

[1] Beutler E, Yoshida A. Human glucose-6-phosphate dehydrogenase variants[J]. Annals of Human Genetics, 2012, 41(2):347-355.

[2] Paglia D E . Acute episodic hemolysis in the African black rhinoceros as an analogue of human glucose-6-phosphate dehydrogenase deficiency.[J]. American Journal of Hematology, 2010, 42(1):36-45.

[3] Wei X , Kixmoeller K , Baltrusaitis E , et al. Allosteric role of a structural NADP+ molecule in glucose-6-phosphate dehydrogenase activity[J]. Proceedings of the National Academy of Sciences of the United States of America. 2022(29):119.

[4] Beutler E, Beutler E. Study of glucose-6-phosphate dehydrogenase: History and molecular biology[J]. American Journal of Hematology, 2010, 42(1):53-58.

[5] Bhageria V , Chowdhury I , Goel N , et al. Anaesthetic management of a patient with glucose-6-phosphate dehydrogenase deficiency undergoing robotic-assisted laparoscopic radical prostatectomy[J]. Journal of Society of Anesthesiologists of Nepal, 2016, 3(2):93.

[6] Cappellini MD, Fiorelli G . Glucose-6-phosphate dehydrogenase deficiency. Lancet[J]. Journal of Pediatrics, 2008, 371(9606):64-74.

[7] Ryan K , Tekwani B L . Current investigations on clinical pharmacology and therapeutics of Glucose-6-phosphate dehydrogenase deficiency[J]. Pharmacology Therapeutics, 2020, 222:107788.

[8] Bancone G , Chu C S . G6PD Variants and Haemolytic Sensitivity to Primaquine and Other Drugs[J]. Frontiers in Pharmacology, 2021, 12:638885.

[9] Manganelli, Genesia, Masullo, et al. Glucose-6-Phosphate Dehydrogenase Deficiency: Disadvantages and Possible Benefits[J]. Cardiovascular & Haematological Disorders -

Drug Targets(Formerly Current Drug Targets - Cardiovascular & Hematological Disorders), 2013.

[10] Sc J , Hirsh J B , Gruchy G . Erythrocyte and platelet glucose 6-phosphate dehydrogenase in normal and mutant caucasians.[J]. Scandinavian Journal of Haematology, 2010, 6(1):5-9.

[11] Patra K C , Hay N . The pentose phosphate pathway and cancer[J]. Trends in Biochemical Sciences, 2014, 39(8):347-354.

[12] Stincone A , Prigione A , Cramer T , et al. The return of metabolism: biochemistry and physiology of the pentose phosphate pathway[J]. Biological Reviews, 2015, 90(3):927-963.

[13] Deng B , Ghatak S , Sarkar S , et al. Novel Bacterial Diversity and Fragmented eDNA Identified in Hyperbiofilm-Forming Pseudomonas aeruginosa Rugose Small Colony Variant[J]. iScience, 2020, 23(2).

[14] Pande V , Ramos M J . Pande, V and Ramos, MJ. Nuclear factor kappa B: a potential target for anti-HIV chemotherapy. Curr Med Chem 10: 1603-1615[J]. Current Medicinal Chemistry, 2003, 10(16):1603-1615.

[15] Masry M E , Ghosh N , Smith J , et al. Aurine Tricarboxylic Acid (ATA) Disrupts DNase-resistant Wound Biofilm Formed By Persister Clinical Isolate Bacteria[J]. Wound repair and regeneration: official publication of the Wound Healing Society [and] the European Tissue Repair Society, 2021(29-3).

[16] Feller S E , Zhang Y , Pastor R W , et al. Constant pressure molecular dynamics simulation: The Langevin piston method[J]. Journal of Chemical Physics, 1995, 103(11):4613-4621.

[17] L Martínez, Andrade R , Birgin E G , et al. Software News and Update Packmol: A Package for Building Initial Configurations for Molecular Dynamics Simulations[J]. Journal of Computational Chemistry, 2009, 30(13):2157-2164.

[18] Horikoshi N , Hwang S , Gati C , et al. Long-range structural defects by pathogenic mutations in most severe glucose-6-phosphate dehydrogenase deficiency[J]. Proceedings of the National Academy of Sciences, 2021, 118(4):e2022790118.

[19] Stanton R C . Glucose-6-phosphate dehydrogenase, NADPH, and cell survival.[J]. Iubmb Life, 2012, 64(5):362-369.

[20] Wang X T , Engel P C . Clinical mutants of human glucose 6-phosphate dehydrogenase: Impairment of NADP+ binding affects both folding and stability[J]. BBA - Molecular Basis of Disease, 2009, 1792(8):804-809.